Journal of
Nanoelectronics and Optoelectronics
Vol. 10, 1–6, 2015

Transmission and Temperature Sensing Characteristics of a Binary and Ternary Photonic Band Gap

Arafa. H. Aly[1,*], S. E.-S. Abdel Ghany[2], M. M. Fadlallah[2], F. E. Salman[2], and B. M. Kamal[2]

[1] *Physics Department, Faculty of Sciences, Beni-suef University, Egypt*
[2] *Physics Department, Faculty of Sciences, Benha University, Egypt*

In this paper, based on the transfer matrix method, the transmission properties in the infrared (IR) region for one-dimensional binary and ternary photonic crystals under the effect of temperature variations have been theoretically studied. Both thermal expansion effect and thermo-optical effect are considered simultaneously. The numerical results show that the photonic band gap can be significantly enlarged compared to the photonic band gap at room temperature. Furthermore, the calculated transmission characteristics in the wavelength domain demonstrate that, ternary structure has a significant effect in the width of the photonic band gap compared to the usual binary photonic crystals. The roles played by the related parameters, such as the thickness of the constituent materials will be discussed and illustrated.

Keywords: Photonic Band Gap, Transfer Matrix Method, Thermo-Optical, Transmission.

RESEARCH ARTICLE

1. INTRODUCTION

In the last decades, a new class of materials had been discovered which have the ability to control the optical properties of materials. Such new materials have been called the photonic materials. They are now known as the photonic crystals (PCs). PCs are periodic, dielectric, and composite structures in which the interfaces between the dielectric media behave as light scattering centers. In general, PCs can be classified into three types, i.e., the one dimensional (1D), the two dimensional (2D) and the three dimensional (3D) PCs.[1–5] The common property among these three types of PCs is the existence of some photonic band gaps (PBGs) in which an electromagnetic wave with certain frequency within one of the PBGs is prohibited to propagate through the structure.[6,7] Owing to the appearance of the PBG, PCs have inspired great interest of researchers from both fundamental and practical viewpoints in optical devices during the last two decades.[8–10]

A large PBG is the cornerstone for various applications such as the omnidirectional high reflector,[10] high-Q microcavities,[11] optical switches,[13] and optical transistors.[14] Once the PC has been fabricated, the optical properties of PCs remain unaltered.

Reliance to this fact, many attempts had been operated for changing the width and the optical properties of the PBGs especially in 1D and 2D PCs. In 1D PCs, ternary structures have a great influence on the properties of the PBGs as compared to binary structures.[15–18] In addition, thermal or thermo-optical effects have a tremendous effects on the PBG properties of 1D structure due to the influence of temperature on the properties of the constituent materials of PCs.[19,20] This effect comes in the form of changes within the refractive indices and the thicknesses of these materials. The changes within these parameters have a great effect on the value of the central frequency of the PBGs of PCs.

In this paper, we tend to modify the IR-transmission characteristics in a 1D binary PCs by adding a third sandwiched between the two constituent dielectric media, giving rise to a 1D ternary PCs from which its PBG can be significantly enhanced. Moreover, the effects of temperature on the width of the PBG and the transmission properties depending on the remarkable effect of the temperature on the thicknesses and the refractive indices of the constituent materials have been demonstrated. From the numerical analysis, many applications in IR region such as electromagnetic waves sensor, optical switches, and filters can be designed.

2. THEORETICAL MODEL

Let us consider a 1D binary PCs which is modeled as an N-period layered structure shown in Figure 1, in which each period has two constituent layers. The refractive indices and thicknesses of the two dielectric layers are

*Author to whom correspondence should be addressed.

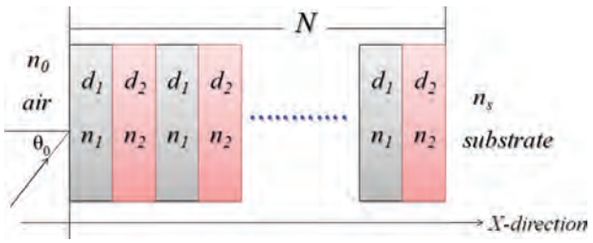

Fig. 1. Schematic diagram of 1D-binary structure; the thicknesses of its constituent materials are denoted by d_1 and d_2, respectively, and the corresponding refractive indices are separately indicated by n_0, n_1, n_2, and n_s, where n_0 is the index of the air and n_s is the index of substrate.

denoted by d_1, d_2 and n_1, n_2, respectively. In the other hand, the ternary structure is designed by sandwiching a third dielectric layer between the two dielectric layers in binary structure as shown in Figure 2. The refractive index and thickness of this dielectric layer are denoted by n_d and d_d, respectively. The binary and the ternary structures are situated between the vacuum and the substrate. For the dielectric media, their values of refractive indices n_1, n_2, and n_d are available in Ref. [21].

The optical properties, such as the wave reflection and transmission, for a 1D binary and ternary periodic layered system can be calculated based on an elegant transfer matrix method (TMM), and the Abeles theory (AT).[22] According to AT, the single period characteristic takes the following form for binary structure:

$$M(a) = \begin{pmatrix} m_{11} & m_{12} \\ m_{21} & m_{22} \end{pmatrix} = \begin{pmatrix} \cos\beta_1 & \frac{-i}{p_1}\sin\beta_1 \\ -ip_1\sin\beta_1 & \cos\beta_1 \end{pmatrix} \times \begin{pmatrix} \cos\beta_2 & \frac{-i}{p_2}\sin\beta_2 \\ -ip_2\sin\beta_2 & \cos\beta_2 \end{pmatrix} \quad (1)$$

Since $a = (d_1 + d_2)$ is the lattice constant. The elements m_{11}, m_{12}, m_{21} and m_{22} were computed by using the following equations:

$$m_{11} = \cos\beta_1\cos\beta_2 - \frac{p_2}{p_1}\sin\beta_1\sin\beta_2 \quad (2\text{–a})$$

$$m_{12} = \frac{-i}{p_1}\sin\beta_1\cos\beta_2 - \frac{i}{p_2}\cos\beta_1\sin\beta_2 \quad (2\text{–b})$$

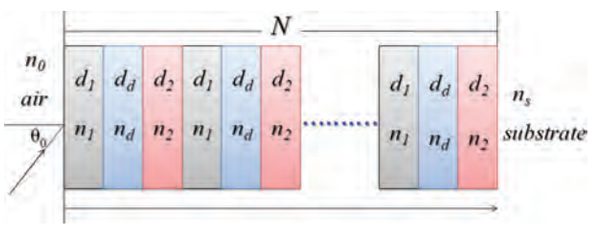

Fig. 2. Schematic diagram of 1D-ternary structure, in which the thicknesses of the three constituent layers are denoted by d_1, d_2, and d_d. The corresponding refractive indices are separately indicated by n_o, n_1, n_2, n_d, and n_s, where $n_o = 1$ is taken for free space and n_s is for the substrate.

$$m_{21} = -ip_1\sin\beta_1\cos\beta_2 - ip_2\cos\beta_1\sin\beta_2 \quad (2\text{–c})$$

$$m_{22} = \cos\beta_1\cos\beta_2 - \frac{p_1}{p_2}\sin\beta_1\sin\beta_2 \quad (2\text{–d})$$

Where:-

$$\beta_1 = \frac{2\pi d_1}{\lambda}n_1\cos\theta_1, \quad \beta_2 = \frac{2\pi d_2}{\lambda}n_2\cos\theta_2 \quad (3)$$

and,

$$p_1 = n_1\cos\theta_1, \quad p_2 = n_2\cos\theta_2 \quad (4)$$

*f*or TE wave, whereas

$$p_1 = \frac{\cos\theta_1}{n_1}, \quad p_2 = \frac{\cos\theta_2}{n_2} \quad (5)$$

*f*or TM wave.

For a system of N periods the total characteristic matrix $M(Na)$ can be obtained using the same expressions which are used in Eq. (2). The reflection coefficient r and the transmission coefficient t, can be written as:

$$r = \frac{(M_{11} + M_{12}f_s)f_0 - (M_{21} + M_{22}f_s)}{(M_{11} + M_{12}f_s)f_0 + (M_{21} + M_{22}f_s)} \quad (6\text{–a})$$

$$t = \frac{2f_0}{(M_{11} + M_{12}f_s)f_0 + (M_{21} + M_{22}f_s)} \quad (6\text{–b})$$

Where, the expressions for f_0 and f_s are defined as following:-

$$f_0 = \sqrt{\frac{\varepsilon_0}{\mu_0}}n_0\cos\theta_0 \quad \text{and} \quad f_1 = \sqrt{\frac{\varepsilon_0}{\mu_0}}n_s\cos\theta_s \quad (7)$$

Finally the reflectance and the transmittance are given by

$$R = |r^2|, \quad T = \frac{f_s}{f_0}|t^2| \quad (8)$$

While for ternary structure, we have:-

$$M(a) = \begin{pmatrix} m_{11} & m_{12} \\ m_{21} & m_{22} \end{pmatrix} = \begin{pmatrix} \cos\beta_1 & \frac{-i}{p_1}\sin\beta_1 \\ -ip_1\sin\beta_1 & \cos\beta_1 \end{pmatrix} \times \begin{pmatrix} \cos\beta_d & \frac{-i}{p_d}\sin\beta_d \\ -ip_d\sin\beta_d & \cos\beta_d \end{pmatrix} \times \begin{pmatrix} \cos\beta_2 & \frac{-i}{p_2}\sin\beta_2 \\ -ip_2\sin\beta_2 & \cos\beta_2 \end{pmatrix} \quad (9)$$

Where $M(a)$ is the matrix for one period and $a = (d_1 + d_d + d_2)$ is the lattice constant. The elements m_{11}, m_{12}, m_{21} and m_{22} *were* calculated by:

$$m_{11} = (\cos\beta_1\cos\beta_d\cos\beta_2) - \frac{p_d}{p_1}(\sin\beta_1\sin\beta_d\cos\beta_2) - \frac{p_2}{p_d}(\cos\beta_1\sin\beta_d\sin\beta_2) - \frac{p_2}{p_1}(\sin\beta_1\cos\beta_d\sin\beta_2) \quad (10\text{–a})$$

RESEARCH ARTICLE

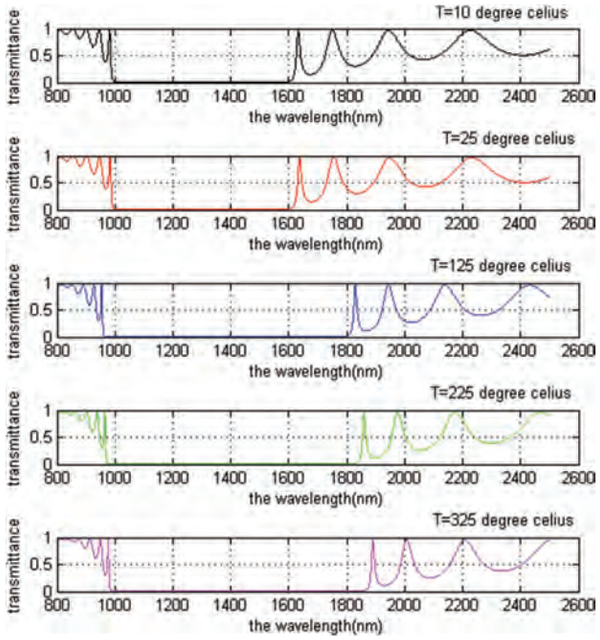

Fig. 3. Transmission spectra for 1D binary Si/SiO_2 PBG structure for $d_1 = 117$ nm and $d_2 = 150$ nm at different values of $\Delta T = 10$ °C, 25 °C, 125 °C, 225 °C and 325 °C, respectively.

$$m_{12} = \frac{ip_d}{p_1 p_2}(\sin\beta_1 \sin\beta_d \sin\beta_2) - \frac{i}{p_1}(\sin\beta_1 \cos\beta_d \cos\beta_2) - \frac{i}{p_d}(\cos\beta_1 \sin\beta_d \cos\beta_2) - \frac{i}{p_2}(\cos\beta_1 \cos\beta_d \sin\beta_2) \quad (10\text{–b})$$

$$m_{21} = \frac{ip_1 p_2}{p_d}(\sin\beta_1 \sin\beta_d \sin\beta_2) - ip_1(\sin\beta_1 \cos\beta_d \cos\beta_2) - ip_d(\cos\beta_1 \sin\beta_d \cos\beta_2) - ip_2(\cos\beta_1 \cos\beta_d \sin\beta_2) \quad (10\text{–c})$$

$$m_{22} = (\cos\beta_1 \cos\beta_d \cos\beta_2) - \frac{p_1}{p_d}(\sin\beta_1 \sin\beta_d \cos\beta_2) - \frac{p_d}{p_2}(\cos\beta_1 \sin\beta_d \sin\beta_2) - \frac{p_1}{p_2}(\sin\beta_1 \cos\beta_d \sin\beta_2) \quad (10\text{–d})$$

Table I. The dependence of the PBG width on the temperature at $d_2 =$ 150 nm for 1D binary structure.

Temperature (in °C)	Width of PBG (in nm)
10	600
25	600
125	840
225	850
325	860

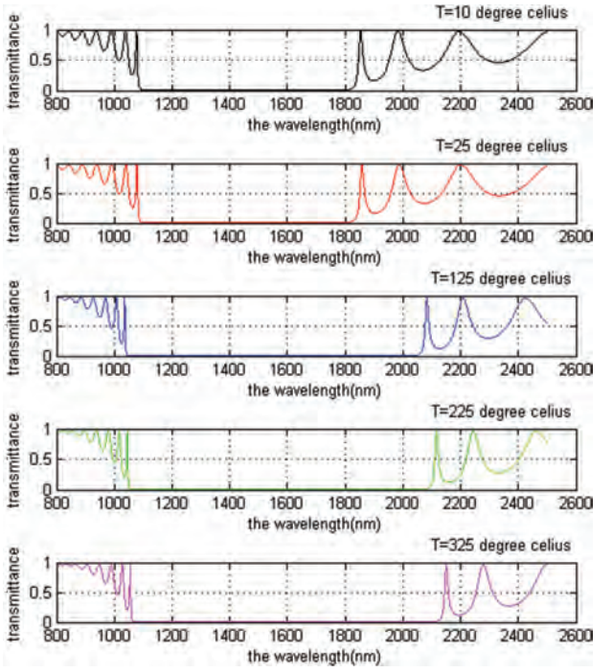

Fig. 4. Transmission spectra for 1D binary Si/SiO_2 PBG structure with $d_1 = 117$ nm, $d_2 = 200$ nm and $N = 10$ at $\Delta T = 10$ °C, 25 °C, 125 °C, 225 °C and 325 °C respectively.

Where:-

$$\beta_j = \frac{2\pi d_j}{\lambda} n_j \cos\theta_j, \quad j = 1, d, 2, \quad (11)$$

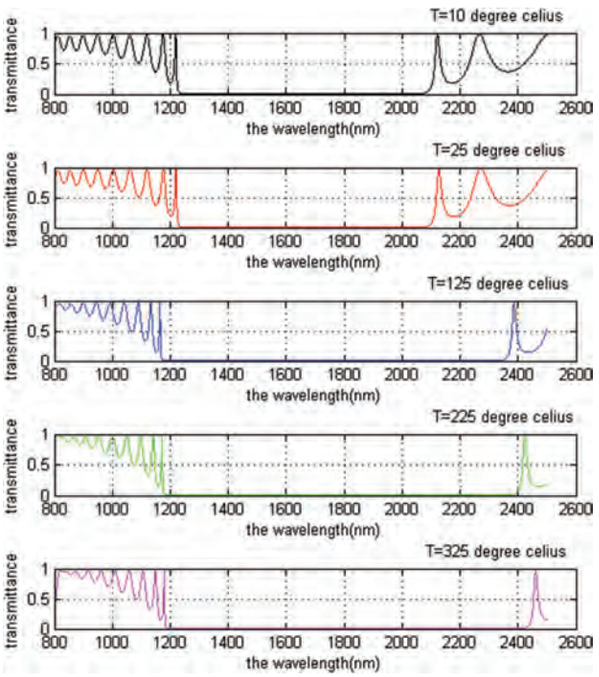

Fig. 5. Transmission spectra for 1D binary Si/SiO_2 PBG structure with $d_1 = 117$ nm, $d_2 = 265$ nm and $N = 10$ at $\Delta T = 10$ °C, 25 °C, 125 °C, 225 °C and 325 °C respectively.

RESEARCH ARTICLE

Table II. The dependence of the PBG width on the temperature at $d_2 = 200$ nm for 1D binary structure.

Temperature (in °C)	Width of PBG (in nm)
10	700
25	700
125	1000
225	1010
325	1020

and

$$p_j = n_j \cos\theta_j \quad \text{for TE-waves}$$
$$p_j = \frac{\cos\theta_j}{n_j} \quad \text{for TM-waves, } j = 1, d, 2 \tag{12}$$

Then the matrix for the whole structure can be obtained by the same method which is used for binary structure.

To include the effect of temperature, it well known that the thickness and the refractive index can be changed due to thermal expansion effect and the thermo-optic effect as follows:-[23]

$$d = d_o + \alpha d_o \Delta T \tag{13}$$

where (d_o) is the thickness of the layer at room temperature, α is the thermal expansion coefficient of the medium and ΔT is the variation of the temperature. The refractive index of the medium *is depend*s on temperature according the thermo-optical effect as follows,

$$n = n_o + \beta n_o \Delta T \tag{14}$$

Where n_o is the refractive index at room temperature and β is the thermo-optic coefficient. Then by inserting Eqs. (13), and (14) inside Eqs. (3), (4), (5), (11), and (12), we can obtain the effect of temperature on 1D binary and ternary PCs.

3. RESULTS AND DISCUSSION

We now *tackle* the numerical results of TE wave's propagation through the 1D PCs under IR radiation. We start our analysis by studying the transmittance characteristics of 1D binary PCs as a function of temperature. Here, two different dielectric media, i.e., Si($d_1 = 117$ nm, $n_1 = 3.3$) and SiO_2 ($d_2 = 150$ nm, $n_2 = 1.46$),[21] are taken for our simulation because of the high index contrast between these two materials. In addition, we demonstrate the transmission response at different values of d_2 for different values of temperature. Here, we set the thermo-optic coefficients for Si and SiO_2 are 1.86×10^{-4}/°C and 6.8×10^{-6}/°C, respectively.[21, 22] Then, the thermal expansion coefficients for Si and SiO_2 are 0.5×10^{-6}/°C and 2.6×10^{-6}, respectively. The substrate is taken to be glass with a refractive index of $n_s = 1.5$. The number of periods, $N = 10$, *is* implemented in our results).

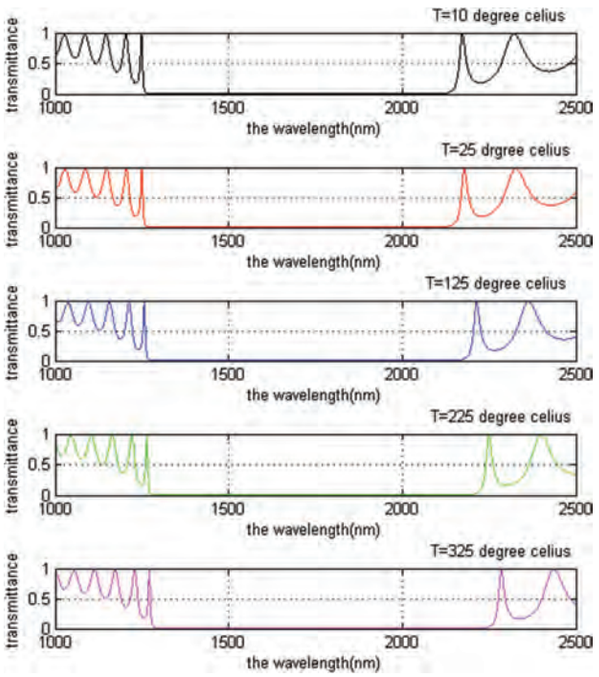

Fig. 6. Transmission spectra for 1D Ternary Si/$Bi_4Ge_3O_{12}$/SiO_2 PBG structure with $d_1 = 117$ nm, $d_d = 10$ nm, $d_2 = 265$ nm, and $N = 10$ at $\Delta T = 10$ °C, 25 °C, 125 °C, 225 °C and 325 °C, respectively.

The calculated normal incidence transmittance spectra of a 1D binary PCs at different values of temperature variations has been shown in Figure 3. It is found that, as the temperature increased 10 °C over the room temperature, there exist a wide PBG within IR region whose bandwidth is 600 nm. This wide PBG may be expected due to the high index contrast between SiO_2 and Si. For further increase in the temperature, the PBG expands towards the far IR due to the increment in the index contrast between SiO_2 and Si as a power result of the thermo-optic effect especially in the high temperature values such as 125 °C, 225 °C, and 325 °C. Table I indicates the transmission response of 1D binary structure through the temperature variations.

Table III. The dependence of the PBG width on the temperature at $d_2 = 265$ nm for 1D binary structure.

Temperature (in °C)	Width of PBG (in nm)
10	840
25	840
125	1150
225	1210
325	1230

Table IV. The dependence of the PBG width on the temperature at $d_2 = 265$ nm, and $d_d = 10$ nm for 1D ternary structure.

Temperature (in °C)	Width of PBG (in nm)
10	866.672
25	866.672
125	916.67
225	966.668
325	1016.666

RESEARCH ARTICLE

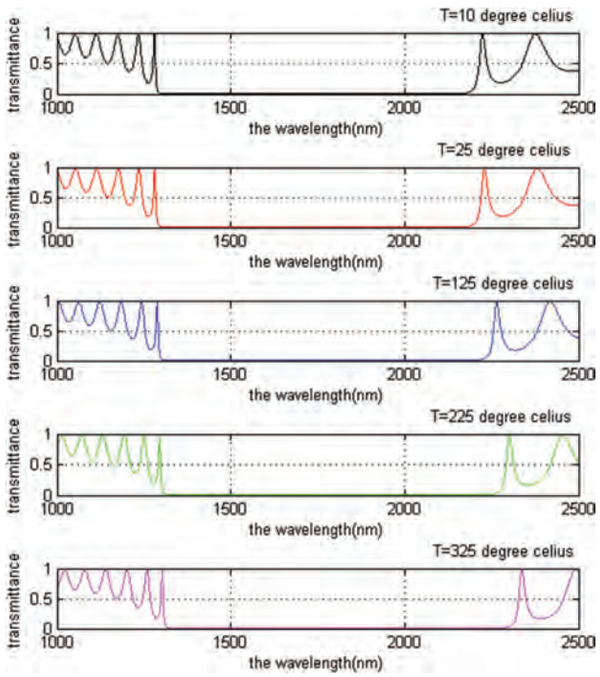

Fig. 7. Transmission spectra for 1D Ternary Si/$Bi_4Ge_3O_{12}$/SiO_2 PBG structure with $d_1 = 117$ nm, $d_d = 20$ nm, $d_2 = 265$ nm and $N = 10$ at $\Delta T = 10$ °C, 25 °C, 125 °C, 225 °C and 325 °C respectively.

To investigate the perfect effect of temperature in the PBG characteristics, we study the dependence of the PBG on the thickness of one of the constituent materials in the presence of temperature variations as shown in

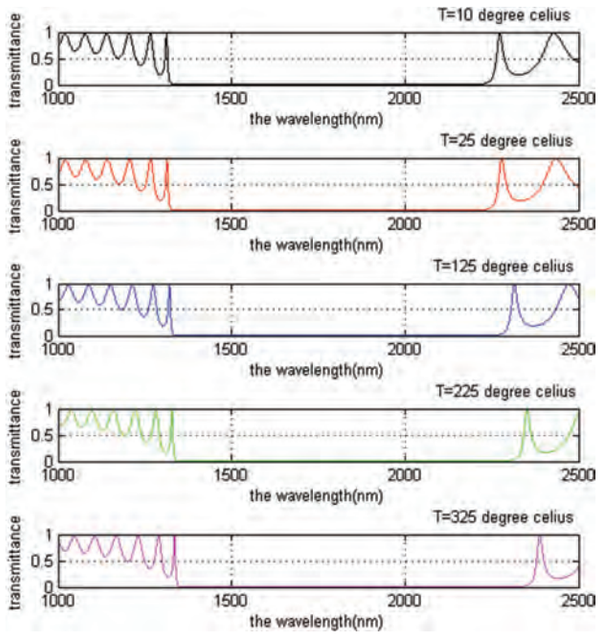

Fig. 8. Transmission spectra for 1D Ternary Si/$Bi_4Ge_3O_{12}$/SiO_2 PBG structure with $d_1 = 117$ nm, $d_A = 30$ nm and $d_2 = 265$ nm, $N = 10$ at $\Delta T = 10$ °C, 25 °C, 125 °C, 225 °C and 325 °C.

Table V. The dependence of the PBG width on the temperature at $d_2 =$ 265 nm, and $d_d = 20$ nm for 1D ternary structure.

Temperature (in °C)	Width of PBG (in nm)
10	883.338
25	908.337
125	950.002
225	2266.656
325	2299.988

Figures 4 and 5. Here, we change the thickness of SiO_2 material only. In comparable with the results investigated in Figure 3, as d_2 increased to 200 nm, the PBG expanded toward the far IR with a remarkable increment in its width to reach 700 nm at $\Delta T = 10$ °C. In addition, the increase in the width of the PBG becomes larger at high values of ΔT as indicated in Table II. This obvious increment in the width of the PBG may be due to the thermal expansion effect which leads to a larger increase in the thickness of the SiO_2 layers as comparable to the state in Figure 3. Then, as d_2 increased to 265 nm, the shift towards the far IR increased with a wider PBG of width 840 nm at $\Delta T =$ 10 °C. This effect stills valid at high values of temperature variations as indicated in Table III.

Turn to the case of 1D ternary PCs in which $Bi_4Ge_3O_{12}$ is sandwiched between Si and SiO_2 to form the ternary structure. Here, we set $n_d = 2.05$, and $d_d = 10$ nm. In addition, the thermo-optic coefficient and the thermal expansion coefficient of $Bi_4Ge_3O_{12}$ are 3.5×10^{-5}/°C and 6.3×10^{-6}/°C, respectively.[21, 22]

The transmittance spectra for 1D ternary structure at normal incidence in the presence of temperature variations has been illustrated in Figure 6. It's seen that, the PBG is shifted more towards the far IR. Furthermore, the width of the PBG increased as comparable to the case of the binary structure to reach 866.672 nm at $\Delta T = 10$ °C. This remarkable increase in the width of the PBG may be due to two reasons. First, the increase in the amount of waves interfering constructively leads to a wider PBG. Second, the influence of temperature to ternary structure is larger than that for binary structure. Then, the width of the PBG stills increase as the temperature variations increase as pronounced in Table IV.

Finally, we investigate in Figures 7, and 8 the dependence of the PBG width on the thickness of $Bi_4Ge_3O_{12}$. At $d_2 = 265$ nm, As the thickness of $Bi_4Ge_3O_{12}$ increases from $d_d = 10$ nm to 20 nm, the PBG raises up to

Table VI. The dependence of the PBG width on the temperature at $d_2 = 265$ nm, and $d_d = 30$ nm for 1D ternary structure.

Temperature (in °C)	Width of PBG (in nm)
10	900.004
25	933.336
125	983.334
225	1049.998
325	1099.996

RESEARCH ARTICLE

883.338 nm and at $d_2 = 265$ nm, $d_d = 30$ nm *at* $d_2 =$ 265 nm, the PBG becomes 900 nm.

By increasing the thickness of $Bi_4Ge_3O_{12}$ layer, it can be seen that the band edge has been significantly moved to the region of far infrared regions, causing the PBG to be widened and consequently to reach the far IR region as elucidated in Tables V and VI.

4. CONCLUSIONS

A theoretical analysis of the transmission properties in IR region for a 1D binary and ternary PCs has been investigated in the presence of temperature variations. It is noted that the temperature variations has a pronounced influence in the PBG structure. The enhancement of PBG can be achieved by increasing the temperature values over the room temperature due to the change in the contrast between the refractive indices of the constituent materials. Furthermore, the width PBG is strongly depending on the thicknesses of the constituent materials. Moreover, the ternary structure has a remarkable effect on the width of the PBG as comparable with binary structure. Using the effect of temperature, we can produce stop bands which may be useful in many applications such as filters and electromagnetic waves sensors.

References and Notes

1. Y. Fink, J. N. Winn, S. Fan, C. Chen, J. Michel, J. D. Joannopoulos, and E. L. Thomas, *Science* 282, 1679 (**1998**).
2. K. Miura, J. Qiu, S. Fujiwara, S. Sakaguchi, and K. Hirao, *Appl. Phys. Lett.* 80, 2263 (**2002**).
3. A. H. Aly and S. W. Ryu, *J. Comput. Theor. Nanosci.* 5, 597 (**2008**).
4. H. Y. Lee and T. Yao, *J. Appl. Phys.* 93, 819 (**2003**).
5. A. H. Aly and H. S. Hanafey, *J. Comput. Theor. Nanosci.* 8, 1916 (**2011**).
6. E. Yablonovich, *Phys. Rev. Lett.* 58, 2059 (**1987**).
7. S. John, *Phys. Rev. Lett.* 58, 2486 (**1987**).
8. A. H. Aly and H. A. Elsayed, *Physica B: Condensed Matter* 407, 120 (**2012**).
9. J. D. Joannopoulos, S. G. Johnson, J. N. Winn, and R. D. Meade, Photonic Crystals: Molding the Flow of Light, Princeton University Press, Princeton, NJ (**1995**).
10. A. H. Aly, H. A. Elsayed, and S. A. El-Naggar, *Accepted and Published Online in Journal of Modern Optics* (**2014**).
11. Z. Y. Li and Y. Xia, *Phys. Rev. B* 64, 1531081 (**2001**).
12. Y. Akahane, T. Asano, B. S. Song, and S. Noda, *Nature* 425, 944 (**2003**).
13. M. F. Yanik, S. Fan, and M. Solijacic, *Appl. Phys. Lett.* 83, 2739 (**2003**).
14. S. John and M. Florescu, *J. Opt. A: Pure Appl. Opt.* 3, S103 (**2001**).
15. S. K. Awasthi and S. P. Ojha, *Prog. In Electromagn. Res. M* 4, 117 (**2008**).
16. A.Banerjee, *Prog. In Electromagn. Res. Lett.* 11, 129 (**2009**).
17. A. Banerjee, *Prog. In Electromagn. Res.* 89, 11 (**2009**).
18. S. Prasad, V. Singh, and A. K. Singh, *Optik* 121, 1520 (**2009**).
19. T. Kai, C. W. Wei, Y. G. Hui, and L. Z. Quan, *Optoelectr. Lett.* 3, 0444 (**2007**).
20. A. Banerjee, *Progr. In Electromag. Resear. Lett.* 11, 129 (**2009**).
21. E. D. Palik, Optical Constants of Solids II, Academic, Boston, MA (**1991**).
22. M. Born and E. Wolf, Principles of Optics, Cambridge, London (**1999**).
23. H. A. Elsayed, S. A. El-Naggar, and A. H. Aly, *J. Mod. Opti.* 61, 385 (**2014**).

Received: 10 October 2014. Accepted: 13 November 2014.

RESEARCH ARTICLE